Steady-state total diffuse reflectance with an exponential decaying source

Panagiotis Symvoulidis,[1,†] Karin M. Jentoft,[1,†] P. Beatriz Garcia-Allende,[1] Jürgen Glatz,[1] Jorge Ripoll,[2] and Vasilis Ntziachristos[1,*]

[1]*Institute for Biological and Medical Imaging, Helmholtz Zentrum München and Technische Universität München, 85764 Neuherberg, Germany*

[2]*Department of Bioengineering and Aerospace Engineering, Universidad Carlos III of Madrid, 28911 Madrid, Spain*

**Corresponding author: symvoulidis@helmholtz-muenchen.de*

Received February 24, 2014; revised May 26, 2014; accepted May 27, 2014; posted May 28, 2014 (Doc. ID 207108); published June 25, 2014

The increasing preclinical and clinical utilization of digital cameras for photographic measurements of tissue conditions motivates the study of reflectance measurements obtained with planar illumination. We examine herein a formula that models the total diffuse reflectance measured from a semi-infinite medium using an exponentially decaying source, assuming continuous plane wave epi-illumination. The model is validated with experimental reflectance measurements from tissue mimicking phantoms. The need for adjusting the blood absorption spectrum due to pigment packaging is discussed along with the potential applications of the proposed formulation.

OCIS codes: (170.3660) Light propagation in tissues; (110.4234) Multispectral and hyperspectral imaging; (170.6935) Tissue characterization.

http://dx.doi.org/10.1364/OL.39.003919

Optical endoscopy is a critical bio-optical method for the diagnosis and management of gastrointestinal conditions and the surgical treatment of various diseases including cancer. Recent interest in fluorescence molecular imaging (FMI) for detection in endoscopic [1] and surgical applications [1,2] further leads to an increasing use of epi-illumination optical imaging in clinical applications.

The optical contrast generated in color endoscopy is due to anatomical features and due to the variation of tissue optical properties. Conversely, in FMI, contrast is generated via the preferential accumulation of an extrinsically administered fluorescent agent to the site of disease. In this case, the fluorescence signals collected depend on the agent concentration in the diseased tissue, the depth of the diseased tissue from the imaged surface, and the tissue optical properties. The collection of color images to capture optical property variation and compensate for their influence on the fluorescence signal has been considered as a method to improve FMI accuracy [3–5]. Both in color endoscopy and in FMI, images are acquired using high-resolution digital cameras [6]. These cameras operate in planar mode, i.e., collecting images emitted back from tissue after tissue illumination with a planar light field.

Herein we sought an analytical formulation that models the dependence of epi-illumination measurements on the underlying tissue optical properties. Such a model is useful to better understand the collected images and provide a forward model for simulation purposes.

Different methods have been already proposed for describing the light collected from tissue in epi-illumination mode, including Monte Carlo simulations or analytical solutions. Monte Carlo approaches are versatile but tend to be computationally expensive and impractical for time-efficient calculations. Alternatively, a set of analytical solutions were proposed by Farrell *et al.* [7], but only for wave and point source illumination, which accounted for an exponentially decaying source (a contribution that in radiative transport theory is termed the reduced intensity, equivalent to Beer's-law [8]). Those formulas has been extensively used in most spatially resolved reflectance measurements (either with a single fiber probe [9], a pair of source-detector probes [10] for single spectrum measurement, or with more pairs [11], or CCD camera pixels as detectors [12] in "imaging" applications) for the determination of optical properties or for elucidating responses from structured illumination patterns [13]. Due to the fact that, to the best of our knowledge, most fluorescence or reflectance measurements have been performed with the use of point sources, the plane wave solution of Farrell has thus received very little attention.

In this work, we employed an alternative expression of Farrell's plane wave formula that introduces plane wave illumination with an exponentially decaying source in order to account for homogeneous or planar illumination scenarios. Derived in the spatial frequency domain, this formulation includes the contribution of the reduced intensity to the diffuse intensity [8], and the absorption dependence on the diffusion coefficient [14]. This new formulation allows the inclusion of arbitrary source profiles without the need to resort to the extrapolated boundary condition, thus maintaining the exponentially decaying contribution [15]. In this way, the proposed expression is more versatile and can be used for application with arbitrary illumination distributions, once its validity is proven against Monte Carlo simulations and Farrell's derivation for the source profiles considered by the latter. Importantly we opted to validate its performance in the visible and to examine whether it could be employed for measurements in color endoscopy, i.e., using cameras in the visible light spectrum. This theoretical study was followed by experimental measurements from phantoms. In order to account for the reduced intensity contribution, we introduce an exponentially decaying source. Assuming illumination with a plane wave, the flux J_{det} that traverses outward from diffusive medium into a nonscattering medium is defined by the boundary condition at

the interface $z = 0$ as (see [16] for a detailed derivation)

$$J_{\text{det}}(z = 0) = \frac{U(z = 0)}{\alpha}, \tag{1}$$

with α representing the boundary coefficient, which accounts for the difference in refractive indices (note that $\alpha = 2$ in the index-matched case), and U represents the average intensity (in Watts/cm^2) at the interface and accounts for the diffusive contribution. If we now take into account an exponentially decaying intensity due to the reduced intensity contribution inside the diffusive medium and consider the effect of the boundary condition shown above, we may obtain, after a straightforward but lengthy derivation (see [15], Chap. 7 and 8), an expression for the average intensity as

$$U(z = 0) = \frac{\text{NA}^2 S_0 \mu_s'}{2\sqrt{D\mu_a}} \frac{1}{\mu_s' + \mu_a + \sqrt{\mu_a/D}} \frac{2\alpha D}{\sqrt{D/\mu_a} + \alpha D}, \tag{2}$$

where NA is the numerical aperture of the lens, S_0 is the power per area that reaches the diffusive medium (in Watts/cm^2), μ_a and μ_s' are the absorption and reduced scattering coefficients, respectively, and D is the diffusion coefficient, which we will define as

$$D = \frac{1}{3(\mu_s' + a\mu_a)}, \tag{3}$$

with a representing a coefficient, which accounts for the absorption dependence of the diffusion coefficient following [17]. Typical values of a range from 0.2 to 0.5. Since S_0 represents the power that reaches the diffusive medium, we may account for the power lost to specular reflection and express S_0 in terms of the total power per area incident on the interface as

$$S_0 = (1 - R_{\text{air}\to n0}) S^{(\text{inc})}, \tag{4}$$

where $R_{\text{air}\to n0} = (n_{\text{air}} - n0/n_{\text{air}} + n0)^2$ is the reflectance going from air into the diffusive medium of index of refraction n_0, and $S^{(\text{inc})}$ is the total power per area incident on the interface. Regrouping terms and introducing these relations, we may rewrite the expression for the detected flux as

$$J_{\text{det}}(z = 0) = \frac{(1 - R_{\text{air}\to n0}) S^{(\text{inc})} \mu_s' \sqrt{D\mu_a}}{\left((\mu_s' + \mu_a)\sqrt{D\mu_a} + \mu_a\right)\left(1 + \alpha\sqrt{D\mu_a}\right)}. \tag{5}$$

Note that this expression assumes a numerical aperture of our detector of NA = 1. As expected, if the semi infinite diffusive medium is nonabsorbing (i.e., $\mu_a = 0$) the total flux reflected would be $J_{\text{det}}(z = 0) = (1 - R_{\text{air}\to n0}) S^{(\text{inc})}$.

We compared Eq. (5) and the Farrell formulation in [7] to a Monte Carlo simulation using the algorithm in [18,19]. In simulations, we assumed a model for steady-state light transport in multilayer tissue [20]. The comparisons assumed typical optical properties for tissue in the visible as previously described [21]. In particular, the simulation was computed for absorption coefficient μ_a values in the range of 0.1–10 cm^{-1} and reduced scattering coefficient μ_s' values in the range of 4–16 cm^{-1}. We assumed that the spectral dependence of μ_a resembled that of blood for different levels of oxygenation varying from 0 to 100%. The spectral dependence of μ_s assumed Mie scattering, i.e., $\mu_s = a * \lambda^{-b}$, with b~2.3. A value of $n_{\text{tissue}} = 1.33$ was used as the refractive index of tissue and g values corresponding to Intralipid 10%, according to Flock *et al.* were utilized [22]. The comparison revealed similar performance for the two analytical equations, resulting in a maximum root-mean-square (RMS) error of 0.69% across the entire visible wavelength range. The RMS error between the epi-illumination predictions offered between Eq. (5) and the Monte Carlo calculation was somewhat larger, resulting in ~2.76%, which nevertheless demonstrated good agreement.

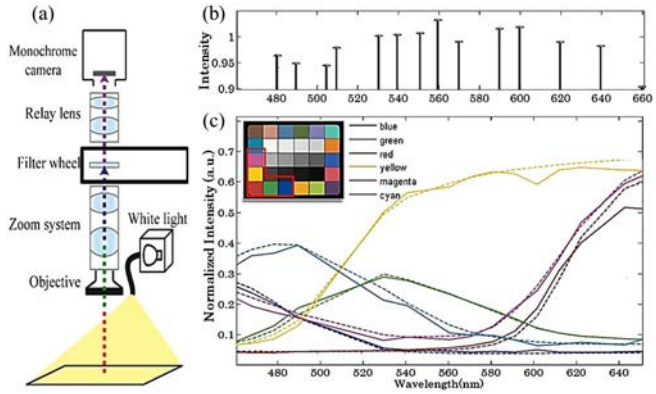

Fig. 1. (a) System schematic. (b) System response (mean measurement from diffuse standard before correction). (c) comparison of measured reflection intensity (solid lines) and documented spectra (dashed lines) of a Macbeth chart.

Due to the agreement observed between analytical and numerical computation, we focused primarily on investigating the agreement between Eq. (5) and experimental measurements. Multispectral reflectance images of aqueous phantoms were acquired with the system shown in Fig. 1(a). The multispectral imaging system mainly consists of a monochromatic camera Luca R (Andor Technology plc, Belfast, UK) employing a 25-position filter-wheel manufactured by Cairn-Research (Kent, UK) and a custom-made casing. 10 nm narrowband filters from Chroma Technology Co. (Bellows Falls, USA) were employed for each waveband of interest [as shown in Fig. 1(b)]. Optical detection was through a Z16 APO A lens (Leica Microsystems GmbH, Wetzlar, Germany) with 1× objective, while white light illumination was provided by a halogen lamp (KL2500, Schott AG, Mainz, Germany). Image acquisition was automated with a custom-developed Labview program (National Instruments, USA), while MATLAB (Ver 2013a Mathworks, USA) was used for data preview and postprocessing.

System calibration was performed in order to compensate for wavelength-dependencies of the camera system. First, dark images were acquired with exposure times that were identical to the epi-illumination images collected. The dark images were subtracted from all the epi-illumination images collected to eliminate DC

offsets. Every epi-illumination image collected through one of the bandpass filters was divided by a corresponding epi-illumination image [mean values shown in Fig. 1(b)] obtained with the same filter, exposure time, and aperture from a diffuse reflectance standard (Ocean Optics, USA), under identical illumination conditions. This division was applied to compensate for filter and illumination specific gains and losses. Figure 1(c) shows the results of the spectral calibration.

The aqueous tissue mimicking phantoms measured consisted of rabbit blood (with the addition of anticlotting agent) with concentrations in the 0.5%–1.94% range using a 0.18% titration step and Intralipid (Sigma-Aldrich, USA) with concentrations in the 0%–5.8% range with a 0.6% titration step. The blood/intralipid solutions were placed in cylinders of ~2 cm radius and ~2.5 cm depth. Since the solution was exposed to air and was well mixed to be as homogeneous as possible before imaging, the hemoglobin is assumed to be fully oxygenated. To compare the experimental results with the output of the proposed formulation [Eq. (5)], we used the absorption spectrum of blood from Oregon Medical Laser Center database (http://omlc.ogi.edu/spectra/) and Intralipid's reduced scattering coefficient as documented in [22].

Figure 2 plots predictions of Eq. (5) against the experimental results collected. It is observed that Eq. (5) accurately predicts the experimental measurements with a mean error of 4.5%, smaller than 10% for all the optical property combinations and across all wavelengths (Fig. 2).

Although the mismatch observed between experimental measurements and theoretical predictions was small, a noticeable correlation with the spectral dependence of hemoglobin extinction coefficients was observed [as seen in Fig. 2(c)]. Accordingly, we investigated the possible sources of error, including a pipetting error and variance

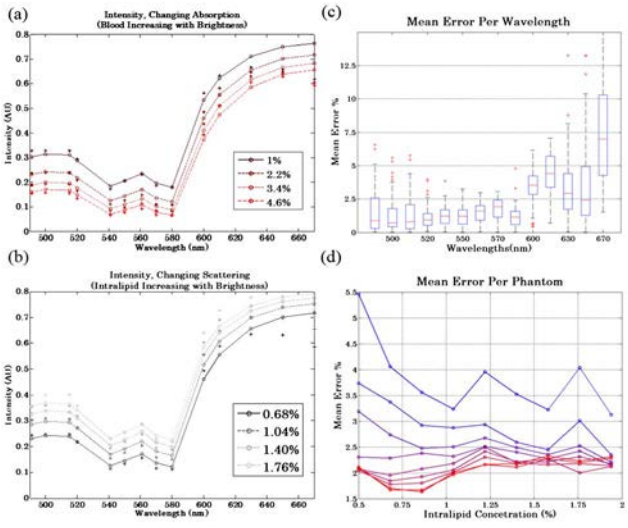

Fig. 2. (a), (b) Comparison of experimental measurements (stars) with theoretical spectral predictions (lines with circles for different blood (a) and Intralipid (b) concentrations. (c) Box plot of the mean error per wavelength for all concentrations (red points: outliers, whiskers: minimum/maximum excluding outliers, box: 25% quartiles; red line: mean value). (d) Mean error per concentration across wavelength (color change from blue to red corresponds to increasing blood concentration).

of expected hemoglobin concentration in the blood. A reasonable explanation that matched our experimental result is in the discussion by Finley [23], regarding the alteration of reflectance spectra of samples containing red blood cells due to pigment packaging effects. Figure 3 compares the blood absorption spectrum as extracted by the fitting of our experimental data with the value given from the formula presented in [22] using the values reported by the authors. This led to significant improvement in matching between experimental measurements and theoretical predictions. Figure 3(b) shows the spectra obtained after incorporating this blood absorption spectrum correction factor (fixed for all the blood concentrations we used) in the formula. Correspondingly, an evenly distributed mean error of 3.9% (12% decrease of error compared with the 4.5% of the uncorrected data) across the whole physiological range of optical properties in the visible wavelengths was found (Fig. 3).

The corrected Eq. (5) demonstrates good agreement with experimental results, pointing to an accurate analytical approach for modeling color CCD camera measurements obtained in epi-illumination mode. The results further imply that despite the diffusion equation approximations, which are better matched in the NIR, the use of Eq. (5) can be efficiently applied in the visible.

Overall, Eq. (5) is a new theoretical formulation of diffuse reflectance, which, in contrast to solutions derived in the past, incorporates arbitrary exponentially decaying sources and describes noncontact planar wave imaging, as performed by clinical cameras. We investigated the

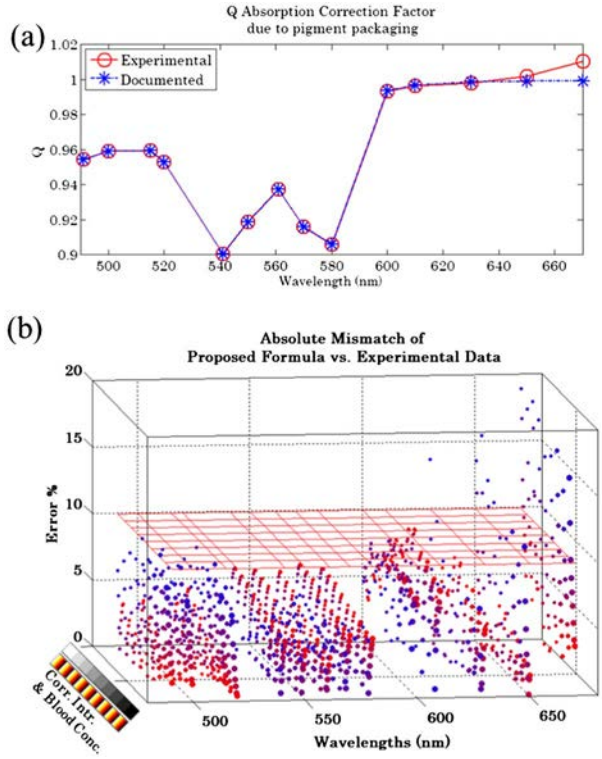

Fig. 3. (a) Comparison of documented and experimentally measured effect of pigment packaging. (b) Absolute error % for all measurements. Marker size: Intralipid conc., marker color (from blue to red): Increasing blood conc. The red horizontal plane thresholds the 10% error.

validity of this formula in modeling responses in the visible range and found it appropriate for predicting epi-illumination measurements for varying optical properties, especially when a correction factor that accounts for pigment packaging effects is incorporated. We further compared Eq. (5) with the existing models and document minor mismatches. Equation (5) therefore provides straightforward implementation for modeling plane wave measurements in the visible range in a quantitative manner and can be used to better interpret measurements obtained by clinical systems in the visible as well.

This research PBGA was supported in part by a Marie Curie Intra European Fellowship within the 7th European Community Framework Program. J. R. acknowledges a Marie Curie CIG grant.

†These authors contributed equally to the work

References

1. P.-L. Hsiung, J. Hardy, S. Friedland, R. Soetikno, C. B. Du, A. P. Wu, P. Sahbaie, J. M. Crawford, A. W. Lowe, and C. H. Contag, Nat. Med. **14**, 454 (2008).
2. G. M. van Dam, G. Themelis, L. M. Crane, N. J. Harlaar, R. G. Pleijhuis, W. Kelder, A. Sarantopoulos, J. S. de Jong, H. J. Arts, and A. G. van der Zee, Nat. Med. **17**, 1315 (2011).
3. W. Scheuer, G. M. van Dam, M. Dobosz, M. Schwaiger, and V. Ntziachristos, Sci. Transl. Med. **4**, 134ps111 (2012).
4. V. Ntziachristos, G. Turner, J. Dunham, S. Windsor, A. Soubret, J. Ripoll, and H. A. Shih, J. Biomed. Opt. **10**, 064007 (2005).
5. R. S. Bradley and M. S. Thorniley, J. R. Soc. Interface **3**, 1 (2006).
6. P. A. Valdés, F. Leblond, A. Kim, B. T. Harris, B. C. Wilson, X. Fan, T. D. Tosteson, A. Hartov, S. Ji, and K. Erkmen, J. Neurosurg. **115**, 11 (2011).
7. G. Themelis, J. S. Yoo, K.-S. Soh, R. Schulz, and V. Ntziachristos, J. Biomed. Opt. **14**, 064012 (2009).
8. T. J. Farrell, M. S. Patterson, and B. Wilson, Med. Phys. **19**, 879 (1992).
9. A. Ishimaru, *Wave Propagation and Scattering in Random Media* (Academic, 1978).
10. G. Zonios, J. Bykowski, and N. Kollias, J. Invest. Derm. **117**, 1452 (2001).
11. F. Bevilacqua, A. J. Berger, A. E. Cerussi, D. Jakubowski, and B. J. Tromberg, Appl. Opt. **39**, 6498 (2000).
12. R. X. Xu, B. Qiang, J. J. Mao, and S. P. Povoski, Appl. Opt. **46**, 7442 (2007).
13. F. Fabbri, M. A. Franceschini, and S. Fantini, Appl. Opt. **42**, 3063 (2003).
14. D. J. Cuccia, F. Bevilacqua, A. J. Durkin, F. R. Ayers, and B. J. Tromberg, J. Biomed. Opt. **14**, 024012 (2009).
15. J. Ripoll, D. Yessayan, G. Zacharakis, and V. Ntziachristos, J. Opt. Soc. Am. A **22**, 546 (2005).
16. J. Ripoll, *Principles of Diffuse Light Propagation: Light Propagation in Tissues with Applications in Biology and Medicine* (World Scientific, 2012).
17. R. Aronson, J. Opt. Soc. Am. A **12**, 2532 (1995).
18. R. Aronson and N. Corngold, J. Opt. Soc. Am. A **16**, 1066 (1999).
19. L. Wang, S. L. Jacques, and L. Zheng, Comput. Methods Programs Biomed. **47**, 131 (1995).
20. L. Wang, S. L. Jacques, and L. Zheng, Comput. Methods Programs Biomed. **54**, 141 (1997).
21. E. Alerstam, T. Svensson, and S. Andersson-Engels, J. Biomed. Opt. **13**, 060504 (2008).
22. S. T. Flock, S. L. Jacques, B. C. Wilson, W. M. Star, and M. J. van Gemert, Lasers Surg. Med. **12**, 510 (1992).
23. J. C. Finlay and T. H. Foster, Opt. Lett. **29**, 965 (2004).